cAMP regulates DEP domain-mediated binding of the guanine nucleotide exchange factor Epac1 to phosphatidic acid at the plasma membrane

Sarah V. Consonni[a,1], Martijn Gloerich[a,1], Emma Spanjaard[a,b], and Johannes L. Bos[a,2]

[a]Molecular Cancer Research, Cancer Genomics Center and Center for Biomedical Genetics, University Medical Center Utrecht, 3584 CG, Utrecht, The Netherlands; and [b]Hubrecht Institute–Royal Netherlands Academy of Arts and Sciences and University Medical Center Utrecht, 3584 CT, Utrecht, The Netherlands

Edited* by Tony Pawson, Samuel Lunenfeld Research Institute, Toronto, ON, Canada, and approved January 23, 2012 (received for review October 26, 2011)

Epac1 is a cAMP-regulated guanine nucleotide exchange factor for the small G protein Rap. Upon cAMP binding, Epac1 undergoes a conformational change that results in its release from autoinhibition. In addition, cAMP induces the translocation of Epac1 from the cytosol to the plasma membrane. This relocalization of Epac1 is required for efficient activation of plasma membrane-located Rap and for cAMP-induced cell adhesion. This translocation requires the Dishevelled, Egl-10, Pleckstrin (DEP) domain, but the molecular entity that serves as the plasma membrane anchor and the possible mechanism of regulated binding remains elusive. Here we show that Epac1 binds directly to phosphatidic acid. Similar to the cAMP-induced Epac1 translocation, this binding is regulated by cAMP and requires the DEP domain. Furthermore, depletion of phosphatidic acid by inhibition of phospholipase D1 prevents cAMP-induced translocation of Epac1 as well as the subsequent activation of Rap at the plasma membrane. Finally, mutation of a single basic residue within a polybasic stretch of the DEP domain, which abolishes translocation, also prevents binding to phosphatidic acid. From these results we conclude that cAMP induces a conformational change in Epac1 that enables DEP domain-mediated binding to phosphatidic acid, resulting in the tethering of Epac1 at the plasma membrane and subsequent activation of Rap.

lipid anchor | membrane translocation | small GTPases

Epac1 and Epac2 are cAMP responsive guanine nucleotide exchange factors (GEFs) for the small G protein Rap and are involved in the spatiotemporal regulation of a variety of processes, among others endothelial cell–cell junction modulation, myocardial contraction, and insulin secretion (1). Epac1 and Epac2 are multidomain proteins, comprising an N-terminal regulatory region and a C-terminal catalytic region. The regulatory region contains one (Epac1) or two (Epac2) cAMP-binding domains and a Dishevelled, Egl-10, Pleckstrin (DEP) domain, whereas the catalytic region harbors a CDC25-homology domain for GEF activity, a REM (Ras exchange motif), and a putative RA (Ras association) domain. In the absence of cAMP, Epac adopts an autoinhibitory conformation in which the regulatory region occludes the binding site for Rap, which is relieved upon cAMP binding (2, 3). In addition to activating Epac1, cAMP also induces its translocation to the plasma membrane (PM). This diffusion-driven translocation requires the DEP domain of Epac1 and functions only in the context of the full-length protein, suggesting that a binding site for a PM anchor is provided in its open conformation (4). Both activation and translocation of Epac1 are required for efficient cAMP-induced activation of Rap1 at the PM and for subsequent downstream responses, such as induction of cell adhesion (4). Epac1 can also be recruited to a more clustered localization at the PM, independent of its DEP domain and cAMP binding, through an interaction with activated Ezrin, Radixin, Moesin (ERM) proteins. This translocation is regulated by ERM-activating stimuli, such as thrombin, and is mediated by the N-terminal 49-aa residues of Epac1 (5). Other membrane anchors for Epac1 within different cellular compartments have been identified (1); however, the PM anchor for the cAMP-induced, DEP domain-mediated localization is currently unclear.

The DEP domain is a 90-aa residue globular domain, first identified in *Drosophila* Dishevelled, *Caenorhabditis elegans* EGL-10, and mammalian Pleckstrin, and present in a number of mammalian protein families (6–9). Of these, the most extensively studied is the DEP domain of Dishevelled (Dvl), an adaptor protein in Wnt-induced signaling. This DEP domain contains a cluster of exposed basic residues that enables membrane recruitment through interactions with negatively charged phospholipids, such as phosphatidic acid (PA), required for both canonical and noncanonical Wnt signaling (10–14). Additional protein interactions by the DEP domain of Dvl further modulate Wnt signaling, which includes its binding to the μ2 subunit of the AP2 clathrin complex to mediate internalization of the Frizzled receptor (15, 16). Another DEP domain-containing family of proteins is the R7 family of regulators of G protein signaling (RGS). RGS proteins are GTPase-accelerating proteins that facilitate GTP hydrolysis of Gα subunits of heterotrimeric G proteins (reviewed in ref. 17). RGS proteins form stable trimeric complexes in a DEP domain-dependent manner with the Gβ5 subunit and specific membrane anchor proteins, such as members of the syntaxin family of SNARE proteins, R7BP and R9AP (18–22). Moreover, the DEP domain of R7-RGS proteins also enables direct interactions with G protein-coupled receptors (23, 24). These studies point out a DEP domain-mediated selectivity for PM anchors and their involvement in multiple distinct molecular interactions controlling membrane recruitment.

The aim of this study was to identify the anchor at the PM for Epac1 and to elucidate the regulatory mechanism for its DEP domain-mediated translocation. We found that in the presence of cAMP, Epac1, but not Epac1 lacking its DEP domain, directly binds to PA. Importantly, this interaction is regulated by cAMP. Furthermore, cellular depletion of PA prevents cAMP-induced Epac1 translocation and subsequent Rap activation at the PM. Finally, we identified a positively charged residue within a polybasic region in the DEP domain of Epac1 that mediates binding to PA. Combined with a recent observation that cAMP increases solvent exposure of this region of the DEP domain (25), we conclude that a cAMP-induced conformational change enables DEP domain-mediated binding of Epac1 to PA at the PM.

Results

cAMP Regulates the Direct Binding of Epac1 to PA. We have previously shown that cAMP induces the translocation of Epac1 to the PM, a process that requires the DEP domain of Epac1. This domain is present in a number of proteins and shown to bind to phospholipids (10, 26). To investigate whether Epac1, in the

Author contributions: S.V.C., M.G., and J.L.B. designed research; S.V.C., M.G., and E.S. performed research; S.V.C., M.G., and E.S. analyzed data; and S.V.C., M.G., and J.L.B. wrote the paper.

The authors declare no conflict of interest.

*This Direct Submission article had a prearranged editor.

Freely available online through the PNAS open access option.

[1]S.V.C. and M.G. contributed equally to this work.

[2]To whom correspondence should be addressed. E-mail: j.l.bos@umcutrecht.nl.

Downloaded by guest on February 24, 2022

presence of cAMP, binds to phospholipids, we carried out protein–lipid overlay assays. Nitrocellulose membranes onto which a variety of lipids were spotted were incubated with bacterially produced recombinant Epac1 in the presence of 8-pCPT-2'OMe-cAMP (also known as 007), a cAMP analog that selectively activates Epac. We observed binding of Epac1 to PA that was at least four times higher than the binding to other phospholipids (Fig. 1 *A* and *B*). Importantly, an Epac1 mutant lacking the DEP domain (ΔDEP-Epac1) did not bind to PA (Fig. 1 *A* and *B*). A similar preference of Epac1 for binding to PA was observed using a liposome binding assay (Fig. 1*C*). To further study the relative binding affinity of Epac1 to PA, we made use of membranes spotted with increasing concentrations of PA. Epac1 showed clear binding to less than 10 pmol PA, whereas ΔDEP-Epac1 did not show any binding even at the highest concentration of PA (Fig. 1*D*). From these results we conclude that Epac1 binds selectively and directly to PA and that this interaction requires the DEP domain.

We next investigated whether cAMP is required for efficient binding of Epac1 to PA, because cAMP is also required for its PM translocation. To that end, recombinant Epac1 was incubated in the presence or absence of 007 with PA containing membranes. In the absence of 007, no binding of Epac1 to PA could be observed after 5 min of incubation, and only limited binding after prolonged incubation for 30 min. However, in the presence of 007 a clear binding was already observed within 5 min, which was further increased after 30 min of incubation (Fig. 1*E*). These results indicate that cAMP binding increases the affinity of Epac1 for PA and implies that its translocation to the PM results from acquired affinity for PA in its open conformation.

PA Is Required for the cAMP-Induced Translocation of Epac1 to the PM. We next investigated whether PA is indeed required for cAMP-induced tethering of Epac1 to the PM. We therefore inhibited one of the PA-generating enzymes, phospholipase D (PLD), using the PLD inhibitor CAY10593. To monitor PA levels we used the PA-binding domain of the Spo20p protein (Spo20p PABD) linked to GFP. This PA sensor resides in the nucleus owing to a nuclear localization signal, unless it is trapped at the membrane by binding to PA (Fig. 2*A*, *Left*, and ref. 27). In

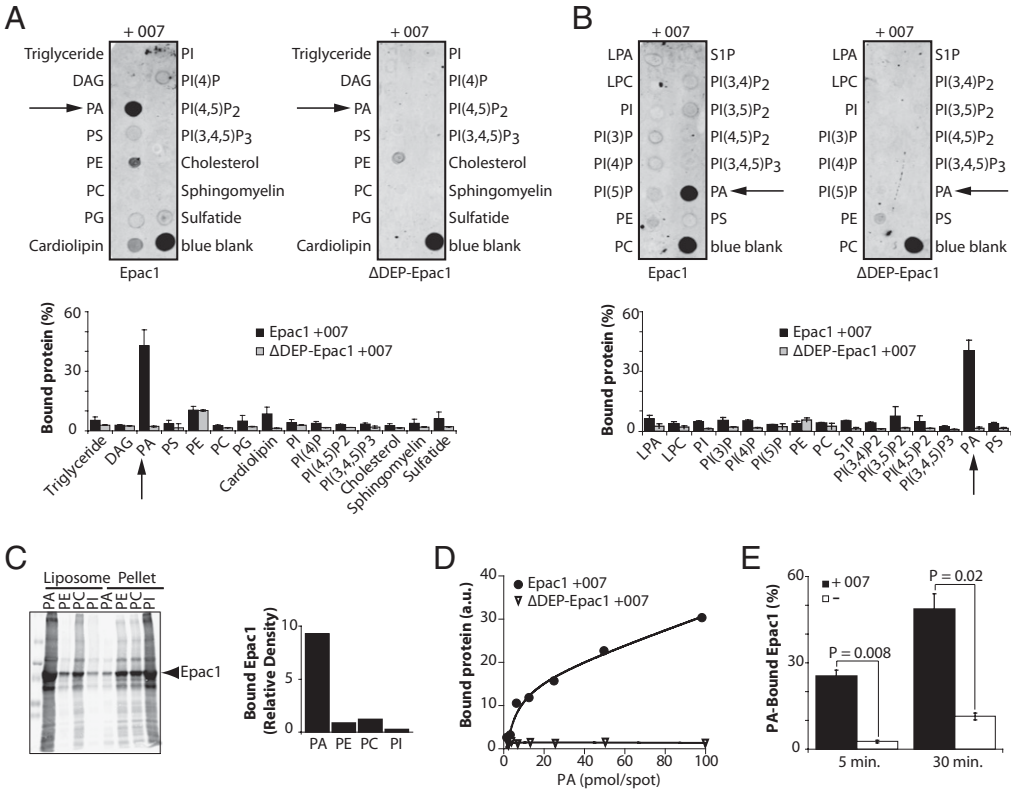

Fig. 1. Epac1 binds to PA in a DEP domain- and cAMP-dependent manner. (*A*) Protein–lipid overlay assay of recombinant Epac1 in the presence of 007 (100 μM) using membrane strips containing 100 pmol/spot of the following lipids: triglyceride, diacylglycerol (DAG), phosphatidic acid (PA), phosphatidylserine (PS), phosphatidylethanolamine (PE), phosphatidylcholine (PC), phosphatidylglycerol (PG), cardiolipin, phosphatidylinositol (PI), phosphatidylinositol 4-phosphate [PI(4)P], phosphatidylinositol 4,5-bisphosphate [PI(4,5)P_2], phosphatidylinositol 3,4,5-trisphosphate [PI(3,4,5)P_3], cholesterol, sphingomyelin, or 3-sulfogalactosylceramide (sulfatide). Binding of Epac1 was detected using the Epac1 antibody 5D3. The bar graph shows the quantification of the binding of Epac1 to the different lipids, showing the mean binding expressed as percentage normalized to control (blue blank) with SD ($n = 3$). (*B*) Protein–lipid overlay assay as in *A* but using PIP strips containing 100 pmol/spot of the following lipids: lysophosphatidic acid (LPA), lysophosphocholine (LPC), PI, phosphatidylinositol 3-phosphate [PI(3)P], PI(4)P, phosphatidylinositol 5-phosphate [PI(5)P], PE, PC, sphingosine 1-phosphate (S1P), phosphatidylinositol 3,4-bisphosphate [PI(3,4)P_2], phosphatidylinositol 3,5-bisphosphate [PI(3,5)P_2], PI(4,5)P_2, PI(3,4,5)P_3, PA, or PS. The bar graph shows the quantification of the binding of Epac1 to the different lipids, showing the mean binding expressed as percentage normalized to control (blue blank) with SD ($n = 3$). (*C*) Epac1 in the presence of 100 μM 8-Br-cAMP was added to liposomes containing PC as the only phospholipid or in addition PA, PE, or PI. Liposomes and bound Epac1 protein were isolated by a sucrose gradient and Epac1 present in the liposome fractions was analyzed by Western blotting. A representative experiment with the quantification of the relative amount of Epac1 in the different liposome fractions (liposome/pellet ratio) is shown. (*D*) Graph showing the representative binding of recombinant Epac1 or ΔDEP-Epac1, in presence of 007 (100 μM), to PA spotted at increasing amounts ranging from 1.56 to 100 pmol/spot onto nitrocellulose membrane. Nonlinear binding curves were fitted using GraphPad Prism software. (*E*) Quantification of the binding of Epac1 to PA, showing the mean binding with SD expressed as percentage normalized to control (blue blank) ($n = 3$). Lipid-containing membrane strips were incubated for the indicated time periods with recombinant Epac1 as in *A*, in the presence or absence of 007 (100 μM), and bound Epac1 was visualized using the Epac1 antibody 5D3. Statistical analysis was performed using a one-tailed Student's *t* test.

Downloaded by guest on February 24, 2022

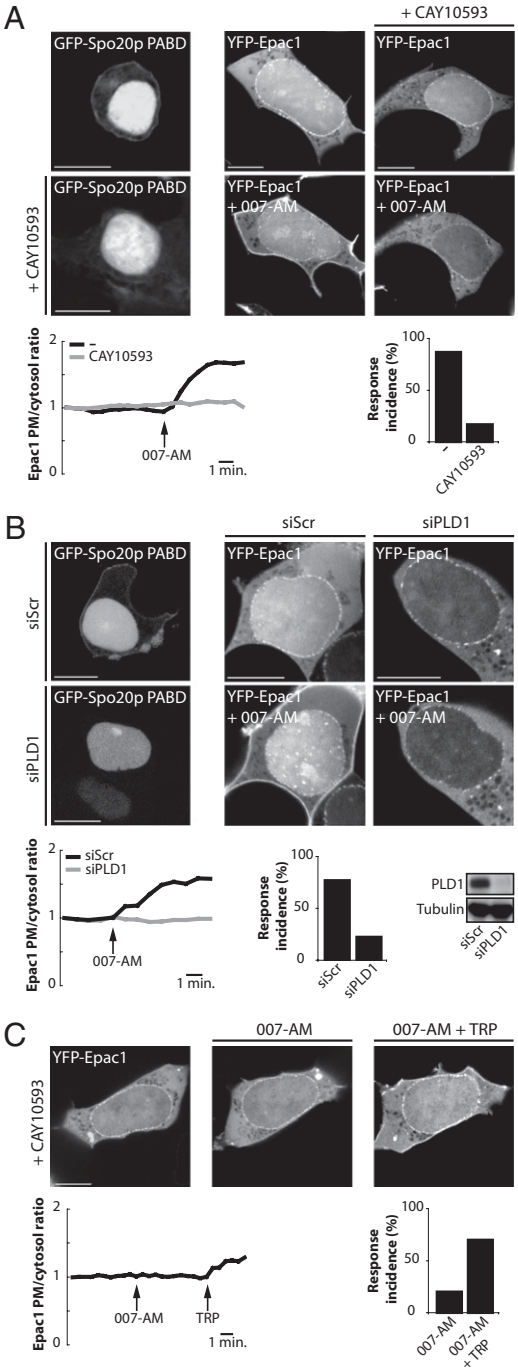

Fig. 2. PA is required for the cAMP-induced translocation of Epac1 to the PM. (*A*) *Left*: Confocal live-imaging of GFP-Spo20p PABD in HEK293T cells, showing its localization at the PM. Treatment of cells with the PLD inhibitor CAY10593 (1 μM) results in PA depletion because it abolishes PM recruitment of GFP-Spo20p PABD. *Right*: Confocal live-imaging of the translocation of YFP-Epac1 to the PM in HEK293T cells by stimulation with 007-AM (1 μM). This translocation of Epac1 is inhibited when cellular PA is depleted by treatment with CAY10593 (1 μM). The graph shows the average fluorescence pixel intensity of YFP-Epac1 at the PM vs. the cytosol during stimulation with 007-AM (1 μM) relative to prestimulus levels, in the absence or presence of CAY10593 (1 μM), calculated as described in *Materials and Methods*. The bar graph shows the percentage of cells showing translocation of Epac1 to the PM upon 007-AM stimulation [response incidence; 13/15 cells expressing YFP-Epac1, and 2/9 cells expressing YFP-Epac1 in the presence of CAY10593 (1 μM)]. (*B*) *Left*: Confocal live-imaging of GFP-Spo20p PABD in HEK293T cells showing its accumulation at the PM in scr siRNA (siScr) transfected cells but not in cells depleted of PLD1 (siPLD1). *Right*: Confocal live-imaging of YFP-Epac1 In HEK293T cells, showing that the 007-AM–induced translocation of YFP-Epac1 observed in siScr transfected cells is lost upon knockdown of PLD1 (siPLD1). The graph shows the average fluorescence pixel intensity of YFP-Epac1 at the PM vs. the cytosol during stimulation with 007-AM (1 μM) relative to prestimulus levels in scr and PLD1 siRNA-transfected cells. The bar graph shows the percentage of cells showing translocation of YFP-Epac1 to the PM upon 007-AM stimulation (response incidence; 10/13 of scr siRNA transfected cells and 2/12 of PLD1 depleted cells). The Western blot shows the efficiency of PLD1 depletion. (*C*) Confocal live-imaging of HEK293T cells depleted of PA by treatment with CAY10593 (1 μM). In the absence of PA, after 007-AM stimulation (1 μM), YFP-Epac1 remains cytosolic but can still be recruited to the PM via activation of ERM proteins by stimulation with TRP (50 μM). The graph shows the average fluorescence pixel intensity of YFP-Epac1 at the PM vs. the cytosol during stimulation with 007-AM (1 μM) and TRP (50 μM) relative to prestimulus levels, in the absence or presence of CAY10593 (1 μM). The bar graph shows the percentage of cells showing translocation of Epac1 to the PM upon 007-AM and TRP stimulation (response incidence; 2/10 cells expressing YFP-Epac1 after 007-AM treatment, and 7/10 cells after TRP stimulation). (Scale bars, 10 μm.)

the presence of CAY10593, PM-bound GFP-Spo20p PABD was no longer observed, indicating that PA in the PM was successfully depleted (Fig. 2*A*, *Left*). Next we examined the translocation of YFP-Epac1 in the presence of this PLD inhibitor. CAY10593 completely abolished the translocation of YFP-Epac1 upon stimulation with 007-AM [a more cell-permeable AM ester of 007 (28)] (Fig. 2*A*, *Right*). To validate the role of PLD in PA formation in HEK293T cells and in Epac1 translocation, we depleted PLD1, the most abundant PLD in these cells (29), using siRNAs. This resulted in loss of Spo20p PABD-GFP from the PM and in inhibition of the cAMP-induced translocation of Epac1 to the PM (Fig. 2*B*).

To exclude that PA depletion from the PM had a more general overall effect on Epac1 translocation, we made use of our previous observation that thrombin receptor stimulation results in the translocation of Epac1 to the PM by a DEP domain-independent mechanism (5). Binding of Epac1 to activated ERM proteins requires the first N-terminal 49-aa residues of Epac1. In cells depleted of PA, thrombin receptor activating peptide (TRP) still induced Epac1 translocation to the PM (Fig. 2*C*). Taken together, we conclude that PA is required for the cAMP-induced membrane translocation of Epac1.

PA Binding Is Needed for Epac1-Mediated Activation of Rap at the PM. We next investigated whether PA is also required for Epac1-mediated activation of Rap at the PM. To that end, we measured the PM recruitment of the YFP-tagged RalGDS Ras/Rap-binding domain (YFP-RalGDS RBD), which recognizes Rap only in its active state (30), upon depletion of PA. We used total internal reflection fluorescence (TIRF) microscopy, which specifically excites fluorophores that are within ≈100 nm of the coverslip, to measure the concentration of fluorescent proteins at the basal cell surface. In control HEK293T cells, 007-AM stimulation resulted in accumulation of both CFP-Epac1 and YFP-RalGDS RBD at the PM (Fig. 3*A*). This was completely abolished when cells were depleted of PA by preincubation with CAY10593. Treatment of cells with TRP after 007-AM stimulation restored PM recruitment of both CFP-Epac1 and YFP-RalGDS RBD (Fig. 3*B*). From these results we conclude that PA is required for Epac1-mediated activation of Rap at the PM.

Arginine 82 Within a Polybasic Stretch in the DEP Domain Is Required for Binding to PA. The DEP domain of Epac1 contains a stretch of 17 residues that includes six basic side-chains (Fig. 4*A*). Because PA binds to positively charged residues at membranes (31), the polybasic cluster in the DEP domain may provide the binding site for PA. One of the residues in this cluster, arginine 82 (R82), was previously found to be essential for cAMP-induced translocation and is in close proximity to a region that becomes more solvent exposed after cAMP binding (Fig. 4 *A* and *B*) (4, 25). To de-

Downloaded by guest on February 24, 2022

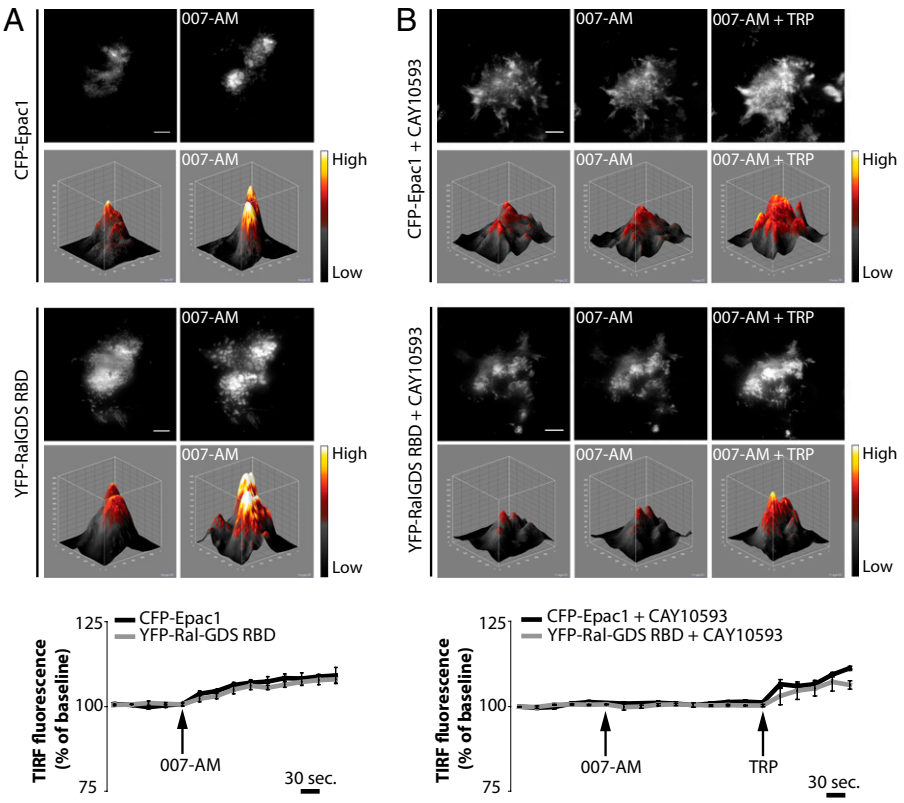

Fig. 3. PA binding is needed for Epac1-mediated activation of Rap at the PM. (*A*) TIRF live-imaging of CFP-Epac1 together with YFP-RalGDS RBD, which binds Rap only in the active conformation, in HEK293T cells. Both Epac1 and RalGDS RBD accumulate at the PM after 007-AM stimulation (1 μM). Representative TIRF images, taken before and after 5-min stimulation with 007-AM, and 3D surface plots (fluorescence intensity of TIRF signal plotted against the surface area of the shown image using the smart lookup table scale) are shown. The graph shows the average fluorescence intensity relative to prestimulus levels with SEM (n = 5). (*B*) Representative TIRF images of CFP-Epac1 and YFP-RalGDS RBD similar to *A*, upon inhibition of cellular PA production by addition of CAY10593 (1 μM), taken before and after 5-min stimulation with 007-AM and following 5-min treatment with TRP. CAY10593 prevents the recruitment of CFP-Epac1 and YFP-RalGDS RBD to the PM after 007-AM (1 μM) stimulation. In contrast, activation of the ERM proteins and DEP-domain independent membrane targeting of Epac1 upon thrombin receptor activation (TRP, 50 μM) results in accumulation of both Epac1 and RalGDS RBD at the PM. The graph shows the average fluorescence intensity relative to prestimulus levels with SEM (n = 5). (Scale bars, 10 μm.)

termine whether the other positively charged side chains within the polybasic stretch of the DEP domain contribute to membrane targeting of Epac1, a series of mutants was analyzed. Some of the mutants displayed reduced response (R85A or R91A), but only the R82A showed a clear inhibition of translocation, as illustrated by both the lack of increased fluorescence at the PM and of response rate (Fig. 4*B*). This indicates that the R82 is the most critical residue for cAMP-induced translocation of Epac1. We therefore tested whether the R82 residue is involved in PA binding, using the protein–lipid overlay assay. Indeed, mutation of arginine 82 to alanine (R82A) completely abolished binding of Epac1 to PA (Fig. 4*C*), indicating that R82 is part of the binding site for PA.

Discussion

We have previously shown that cAMP binding activates Epac1 by releasing it from autoinhibition but also induces its translocation to the PM (2–4, 32, 33). This translocation of Epac1 is required for efficient Rap1 activation and subsequent cell adhesion (4). We now show that Epac1 can bind to PA in vitro in a DEP domain-dependent manner and that this interaction is regulated by cAMP. Depletion of PA by inhibition or depletion of PLD1 abolishes DEP domain-mediated, but not ERM-mediated, recruitment of Epac1. Furthermore, we illustrate that depletion of PA inhibits cAMP-induced activation of Rap at the PM, which can be restored by thrombin-induced tethering of Epac1 to active ERM proteins. Finally, we show that R82 within the DEP domain, which is required for cAMP-induced translocation, is also required for PA binding. Collectively, our results show that PA is the cAMP-regulated DEP domain anchor for Epac1 at the PM.

The observation that cAMP facilitates the binding of PA to the DEP domain suggests that the PA binding site in the DEP domain may become exposed upon the conformational opening of Epac1; however, the crystal structure of Epac2 in its closed conformation indicates that the DEP domain is not sterically hindered by the catalytic region. Furthermore, DEP domain-mediated PM anchoring is only observed in the context of the full protein and not with the individual regulatory region (containing the DEP domain and the cAMP-binding domain) or the isolated DEP domain (4). Possibly, cAMP binding induces additional conformational changes to allow interactions of the DEP domain with PA. Importantly, deuterium exchange mass spectrometry revealed a change in solvent exposed areas in the DEP domain of Epac after cAMP binding, suggesting a cAMP-induced conformational change in the DEP domain (25). Interestingly, the polybasic stretch containing R82 is partially overlapping with the region that became more solvent exposed after cAMP binding (Fig. 4*A*). We therefore propose that cAMP induces a conformational change that induces inter- and intra-domain conformational changes in Epac1 that results in activation of its guanine nucleotide exchange activity but also reorients the loop containing R82, thereby regulating the binding to PA at the PM. However, the presence of a cAMP-induced PA-binding site in the catalytic domain that cooperates with the binding site in the DEP domain is not excluded.

Although PA is distributed uniformally at the PM of most cells, it also contributes to compartmentalization of distinct cellular signaling events (34). For instance, PA enables the correct localization of the RacGEF DOCK2 at the leading edge of neutrophils during chemotaxis (35) and recruits the RasGEF Sos to cell-free membranes but not to cell–cell contact areas (36–38). Although not observed in the cell lines we have studied, it may imply that PA localizes Epac1 to restricted areas of the PM. In this respect, it is interesting to note that several additional membrane anchors for Epac1 have been described (1), indicating a complex spatial regulation of Epac1.

In summary, we show that the DEP domain of Epac1 binds to PA and that this binding is regulated by cAMP. Furthermore we show that PA is required for cAMP-induced translocation and Rap1 activation. This provides further insight into the mechanism of spatiotemporal control of Epac1 and, more generally, into the molecular mechanism of how DEP domains tether proteins to membranes.

Downloaded by guest on February 24, 2022

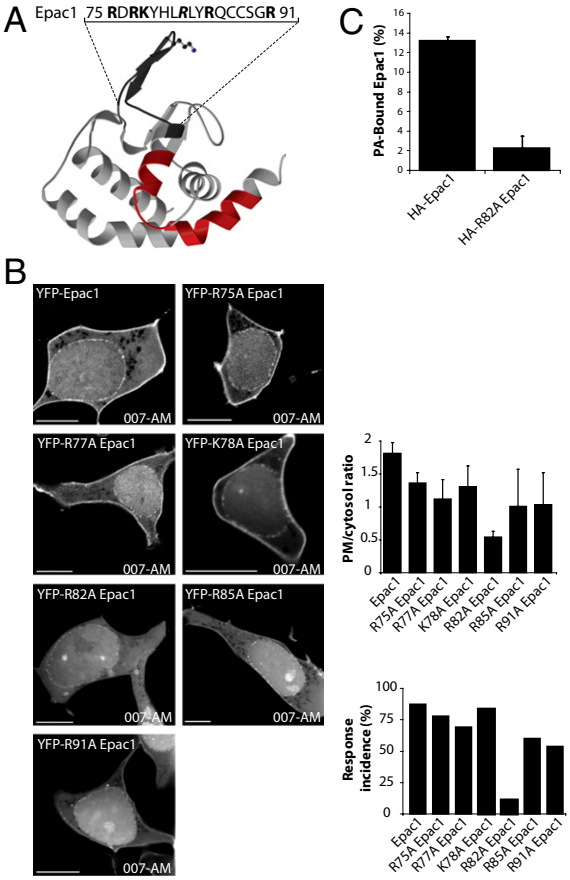

Fig. 4. R82 within a polybasic stretch mediates binding of Epac1 to PA. (*A*) Ribbon diagram of the DEP domain of Epac2 (32) with indicated positively charged residues. Residue K212 in Epac2, corresponding to R82 in Epac1, is presented as ball-and-stick. The region that becomes more solvent exposed after cAMP (25) is highlighted in red, and the amino acid sequence of the cluster of basic residues present in the DEP domain of Epac1 (amino acids 75–91) are shown in dark gray. Positively charged residues are represented in bold, R82 residue in bold italic. (*B*) Confocal live-imaging of HEK293T cells stimulated with 007-AM (1 μM) showing deficient translocation of YFP-R82A Epac1 but not of YFP-R75A Epac1, YFP-R77A Epac1, and YFP-K78A Epac1, and reduced membrane localization of YFP-R85A Epac1 and YFP-R91A Epac1 compared with wild-type YFP-Epac1. The top bar graph shows the average ratio of fluorescence pixel intensity of Epac1 at the PM vs. the cytosol after stimulation with 007-AM (1 μM). The error bars show mean with SD ($n = 4$). The bottom bar graph shows the percentage of cells showing translocation of Epac1 to the PM upon 007-AM stimulation (response incidence; 7/8 cells expressing YFP-Epac1, 7/9 cells expressing YFP-R75A Epac1, 9/13 cells expressing YFP-R77A Epac1, 10/12 cells expressing YFP-K78A Epac1, 1/9 cells expressing YFP-R82A Epac1, 9/15 cells expressing YFP-R85A Epac1, and 7/13 cells expressing YFP-R91A Epac1). (*C*) Quantification of the interaction of wild-type Epac1 and R82A Epac1 with PA. Equal amounts of HA-Epac1 and HA-R82A Epac1 isolated from HEK293T cells were incubated with lipid strips in the presence of 007 (100 μM). Anti-Epac1 5D3 antibody was used to detect binding, and the graph shows percentage of PA-bound Epac1 compared with control (blue blank), showing mean with SD ($n = 3$).

Materials and Methods

Reagents and DNA Constructs. 8-pCPT-2′-O-Me-cAMP (007) and 8-pCPT-2′-O-Me-cAMP-AM (007-AM) were from Biolog Life Sciences; the PLD inhibitor CAY10593 was from Cayman Chemical, and TRP (SFLLRNPDKYEPF sequence) was a kind gift from Kees Jalink (The Netherlands Cancer Institute, Amsterdam, The Netherlands). The PLD1 antibody was from Sigma, the anti-HA antibody was from Covance, and the 5D3 anti-Epac1 antibody has been previously described (39). ON-TARGET plus SMARTpool siRNAs directed against PLD1 (J-009413) and scrambled control siRNAs were from Thermo Scientific Dharmacon. The wild-type Epac1, ΔDEP-Epac1 (amino acids 50–148 deleted), and R82A Epac1 constructs have been described previously (4). Mutations were introduced by site-directed mutagenesis. Purification of recombinant Epac1 and ΔDEP-Epac1 was previously described (40), YFP-RalGDS RBD was kindly provided by Mark Philips (New York University School of Medicine, New York, NY), and GFP-Spo20p PABD was a kind gift from Nicolas Vitale (Institute of Cellular and Integrative Neurosciences, Strasbourg, France).

Cell Culture and Transfection. HEK293T cells were grown in DMEM supplemented with 10% FBS and antibiotics. Cells were transfected with expression plasmids using X-tremeGENE 9 transfection reagent (Roche) and with SMARTpool siRNA using HiPerfect (Qiagen), according to the manufacturer's protocol.

Cell Imaging. For confocal live-imaging, 1 d after transfection cells were seeded overnight in glass-bottom wells (WillCo Wells) in the presence of CAY10593 (1 μM) where indicated, and examined in L-15 Leibovitz medium (Invitrogen) at 37 °C on an inverted Zeiss LSM510 confocal microscope equipped with 63× magnification objective lens (N.A. 1.4; Leica). For TIRF imaging, cells expressing CFP-Epac1 and YFP-RalGDS RBD, preincubated overnight with CAY10593 (1 μM) where indicated, were imaged on a TIRF microscope (Ti; Nikon) with a 60× 1.49 NA Apo TIRF objective lens and an electron microscopy charge-coupled device camera (Luka; Andor) at 37 °C. A series of images were taken at 30-s intervals. For quantification of TIRF microscopy, images were corrected for background, measured in a region of the image that did not contain cells, and the average pixel intensity was measured over time in a region of interest enclosing a cell expressing CFP-Epac1 and YFP-RalGDS RBD and normalized to the start value. For quantification of the translocation of Epac1 constructs, time series images (Fig. 2) or images of cells taken after stimulation with 007-AM (1 μM) (Fig. 4) were imported into a custom-made visual studio program (Professional edition 2008; Microsoft), in which the PM/cytoplasmic fluorescence ratio was measured. Regions of interest at the PM, cytoplasm, and background were determined automatically for every image, and the fluorescence pixel intensity was measured (41).

Protein–Lipid Overlay Assays. Nitrocellulose membranes spotted with a variety of lipids or with increasing amounts of lipids (PIP and Membrane strips and Membrane lipid array; Echelon Biosciences) were blocked for 1 h in 3% fatty acid-free BSA in TBST [50 mM Tris·HCl (pH 7.5), 150 mM NaCl, and 0.1% Tween 20] and then incubated with 1 μg/mL of recombinant full-length His-Epac1 or GST-ΔDEP-Epac1 in presence or absence of 8-pCPT-2′O-Me-cAMP (007, 100 μM) for the indicated time periods. For experiments using Epac1 isolated from HEK293T cells, cells were transfected with HA-Epac1 or HA-R82A Epac1 and then lysed in buffer containing 50 mM Tris·HCl (pH 7.5), 150 mM NaCl, 1% Triton X-100, 2 mM $MgCl_2$, and protease and phosphatase inhibitors. Lysates were then incubated overnight with protein G Sepharose beads and anti-HA antibody. After washing of the beads, the bound proteins were eluted with 3× HA pepetide (250 μg/mL) in BC300 buffer [20 mM Tris·HCl (pH 7.9), 20% glycerol, and 300 mM KCl], and protein recovery was determined by Western blotting. Equal amounts of Epac1 and R82A Epac1 were incubated with lipid strips in the presence of 007 (100 μM). Bound protein was detected using the 5D3 anti-Epac1 antibody and visualized by Odyssey Infrared Imaging (Li-Cor).

Liposome Assay. The liposome binding assay was performed as described previously (42). In brief, liposomes containing phosphatidylcholine (PC) as the only phospholipid or 80% (mol) PC and in addition either 20% PA, phosphatidylethanolamine (PE), or phosphatidylinositol (PI) were made by mixing stock solutions of lipids with cholesterol in a molecular ration of 2.28:1. The chloroform/methanol solvent was evaporated using a flow of N2 with subsequent drying at room temperature in a speedvac (Savant SVC100H) for at least 90 min. Lipids were resuspended in 50-NT buffer [50 mM NaCl and 25 mM Tris·HCl (pH 7.4)] to a final concentration of 6.8 μmol/mL, and liposomes were generated by sonicating on ice using an ultrasonic probe (MSE Soniprep 150). Fifty microliters of the liposome suspension was incubated with 1 μg of recombinant His-Epac1 in 50-NT buffer for 90 min at 37 °C in the presence of 100 μM 8-Br-cAMP. Sucrose [60% (wt/vol)] was mixed with the sample to a final concentration of 36.5%, and samples were overlayed with 500 μL 25% (wt/vol) sucrose in 50-NT buffer and subsequently with 100 μL 50-NT buffer. Subsequently samples were centrifuged in a TLA-55 rotor (Beckman) for 90 min at 136,000 × *g* at 4 °C. After centrifugation, liposome-bound protein was collected in 300 μL from the top of the gradient, and unbound protein was collected in 300 μL from the pellet fraction. Collected proteins were analyzed by SDS/PAGE and Western blotting using the Epac1 5D3 antibody.

Downloaded by guest on February 24, 2022

ACKNOWLEDGMENTS. We thank Holger Rehmann for providing recombinant Epac1 protein and the ribbon diagram of Epac, Marije Rensen for technical assistance, Bernd Helms and Ruud Eerland for help with the liposome binding assay, Jacco van Rheenen for providing the custom-made visual studio program and for help with quantification, Christa Testerink and members of our laboratory for discussions, and Madelon Maurice for critically reading the manuscript. This work is supported by Chemical Sciences (S.V.C. and M.G.) and the Netherlands Genomics Initiative (E.S. and J.L.B.) of the Netherlands Organization for Scientific Research.

1. Gloerich M, Bos JL (2010) Epac: Defining a new mechanism for cAMP action. *Annu Rev Pharmacol Toxicol* 50:355–375.
2. Rehmann H, et al. (2008) Structure of Epac2 in complex with a cyclic AMP analogue and RAP1B. *Nature* 455:124–127.
3. Rehmann H, Das J, Knipscheer P, Wittinghofer A, Bos JL (2006) Structure of the cyclic-AMP-responsive exchange factor Epac2 in its auto-inhibited state. *Nature* 439: 625–628.
4. Ponsioen B, et al. (2009) Direct spatial control of Epac1 by cyclic AMP. *Mol Cell Biol* 29: 2521–2531.
5. Gloerich M, et al. (2010) Spatial regulation of cyclic AMP-Epac1 signaling in cell adhesion by ERM proteins. *Mol Cell Biol* 30:5421–5431.
6. Ballon DR, et al. (2006) DEP-domain-mediated regulation of GPCR signaling responses. *Cell* 126:1079–1093.
7. Civera C, Simon B, Stier G, Sattler M, Macias MJ (2005) Structure and dynamics of the human pleckstrin DEP domain: Distinct molecular features of a novel DEP domain subfamily. *Proteins* 58:354–366.
8. Ponting CP, Bork P (1996) Pleckstrin's repeat performance: A novel domain in G-protein signaling? *Trends Biochem Sci* 21:245–246.
9. Pan WJ, et al. (2004) Characterization of function of three domains in dishevelled-1: DEP domain is responsible for membrane translocation of dishevelled-1. *Cell Res* 14: 324–330.
10. Simons M, et al. (2009) Electrochemical cues regulate assembly of the Frizzled/Dishevelled complex at the plasma membrane during planar epithelial polarization. *Nat Cell Biol* 11:286–294.
11. Boutros M, Paricio N, Strutt DI, Mlodzik M (1998) Dishevelled activates JNK and discriminates between JNK pathways in planar polarity and wingless signaling. *Cell* 94: 109–118.
12. Axelrod JD, Miller JR, Shulman JM, Moon RT, Perrimon N (1998) Differential recruitment of Dishevelled provides signaling specificity in the planar cell polarity and Wingless signaling pathways. *Genes Dev* 12:2610–2622.
13. Wong HC, et al. (2000) Structural basis of the recognition of the dishevelled DEP domain in the Wnt signaling pathway. *Nat Struct Biol* 7:1178–1184.
14. Jung H, et al. (2009) Negative feedback regulation of Wnt signaling by Gbetagamma-mediated reduction of Dishevelled. *Exp Mol Med* 41:695–706.
15. Yu A, et al. (2007) Association of Dishevelled with the clathrin AP-2 adaptor is required for Frizzled endocytosis and planar cell polarity signaling. *Dev Cell* 12:129–141.
16. Yu A, Xing Y, Harrison SC, Kirchhausen T (2010) Structural analysis of the interaction between Dishevelled2 and clathrin AP-2 adaptor, a critical step in noncanonical Wnt signaling. *Structure* 18:1311–1320.
17. De Vries L, Zheng B, Fischer T, Elenko E, Farquhar MG (2000) The regulator of G protein signaling family. *Annu Rev Pharmacol Toxicol* 40:235–271.
18. Anderson GR, Posokhova E, Martemyanov KA (2009) The R7 RGS protein family: Multi-subunit regulators of neuronal G protein signaling. *Cell Biochem Biophys* 54: 33–46.
19. Drenan RM, et al. (2006) R7BP augments the function of RGS7*Gbeta5 complexes by a plasma membrane-targeting mechanism. *J Biol Chem* 281:28222–28231.
20. Kovoor A, et al. (2005) D2 dopamine receptors colocalize regulator of G-protein signaling 9-2 (RGS9-2) via the RGS9 DEP domain, and RGS9 knock-out mice develop dyskinesias associated with dopamine pathways. *J Neurosci* 25:2157–2165.
21. Martemyanov KA, et al. (2003) The DEP domain determines subcellular targeting of the GTPase activating protein RGS9 in vivo. *J Neurosci* 23:10175–10181.
22. Hu G, Zhang Z, Wensel TG (2003) Activation of RGS9-1GTPase acceleration by its membrane anchor, R9AP. *J Biol Chem* 278:14550–14554.
23. Sandiford SL, Slepak VZ (2009) The Gbeta5-RGS7 complex selectively inhibits muscarinic M3 receptor signaling via the interaction between the third intracellular loop of the receptor and the DEP domain of RGS7. *Biochemistry* 48:2282–2289.
24. Sandiford SL, Wang Q, Levay K, Buchwald P, Slepak VZ (2010) Molecular organization of the complex between the muscarinic M3 receptor and the regulator of G protein signaling, Gbeta(5)-RGS7. *Biochemistry* 49:4998–5006.
25. Li S, et al. (2011) Mechanism of intracellular cAMP sensor Epac2 activation: cAMP-induced conformational changes identified by amide hydrogen/deuterium exchange mass spectrometry (DXMS). *J Biol Chem* 286:17889–17897.
26. Hurley JH, et al. (2002) Structural genomics and signaling domains. *Trends Biochem Sci* 27:48–53.
27. Zeniou-Meyer M, et al. (2007) Phospholipase D1 production of phosphatidic acid at the plasma membrane promotes exocytosis of large dense-core granules at a late stage. *J Biol Chem* 282:21746–21757.
28. Vliem MJ, et al. (2008) 8-pCPT-2′-O-Me-cAMP-AM: an improved Epac-selective cAMP analogue. *Chembiochem* 9:2052–2054.
29. Chae YC, et al. (2008) Phospholipase D activity regulates integrin-mediated cell spreading and migration by inducing GTP-Rac translocation to the plasma membrane. *Mol Biol Cell* 19:3111–3123.
30. Bivona TG, Philips MR (2005) Analysis of Ras and Rap activation in living cells using fluorescent Ras binding domains. *Methods* 37:138–145.
31. Kooijman EE, et al. (2007) An electrostatic/hydrogen bond switch as the basis for the specific interaction of phosphatidic acid with proteins. *J Biol Chem* 282:11356–11364.
32. Rehmann H, et al. (2003) Structure and regulation of the cAMP-binding domains of Epac2. *Nat Struct Biol* 10:26–32.
33. Rehmann H, Rueppel A, Bos JL, Wittinghofer A (2003) Communication between the regulatory and the catalytic region of the cAMP-responsive guanine nucleotide exchange factor Epac. *J Biol Chem* 278:23508–23514.
34. van Meer G, Voelker DR, Feigenson GW (2008) Membrane lipids: Where they are and how they behave. *Nat Rev Mol Cell Biol* 9:112–124.
35. Nishikimi A, et al. (2009) Sequential regulation of DOCK2 dynamics by two phospholipids during neutrophil chemotaxis. *Science* 324:384–387.
36. Zhao C, Du G, Skowronek K, Frohman MA, Bar-Sagi D (2007) Phospholipase D2-generated phosphatidic acid couples EGFR stimulation to Ras activation by Sos. *Nat Cell Biol* 9:706–712.
37. Nishioka T, Frohman MA, Matsuda M, Kiyokawa E (2010) Heterogeneity of phosphatidic acid levels and distribution at the plasma membrane in living cells as visualized by a Föster resonance energy transfer (FRET) biosensor. *J Biol Chem* 285: 35979–35987.
38. Zhang Y, Du G (2009) Phosphatidic acid signaling regulation of Ras superfamily of small guanosine triphosphatases. *Biochim Biophys Acta* 1791:850–855.
39. Price LS, et al. (2004) Rap1 regulates E-cadherin-mediated cell-cell adhesion. *J Biol Chem* 279:35127–35132.
40. de Rooij J, et al. (2000) Mechanism of regulation of the Epac family of cAMP-dependent RapGEFs. *J Biol Chem* 275:20829–20836.
41. Leyman S, et al. (2009) Unbalancing the phosphatidylinositol-4,5-bisphosphate-cofilin interaction impairs cell steering. *Mol Biol Cell* 20:4509–4523.
42. Van Galen J, et al. (2010) Binding of GAPR-1 to negatively charged phospholipid membranes: Unusual binding characteristics to phosphatidylinositol. *Mol Membr Biol* 27:81–91.

Downloaded by guest on February 24, 2022